EUROPEAN ORGANIZATION FOR NUCLEAR RSEARCH

CERN PS/87-41 (LPI)

The Model of the Bending Magnets used in the 600 MeV e^+ - e^- Accumulator of LEP

M. Bell, J.P. Delahaye and H. Kugler

A B S T R A C T

Since this accumulator has relatively short bending magnets, the fringe-field effects are large, and special attention had to be paid to the tracking of particles through the magnet as well as to its representation in the machine lattice. Here we describe the procedures, making use of measured field tables in computer programs to determine the properties of the machine, and compare predicted machine parameters with measured ones.

Paper presented at the 1987 IEEE Particle Accelerator Conference

Washington D.C., March 16-19, 1987

Geneva, March 1987

CERN PS/87-41
March 1987

THE MODEL OF THE BENDING MAGNETS USED IN THE 600 MeV e^+-e^- ACCUMULATOR OF LEP

M. Bell, J.P. Delahaye and H. Kugler
CERN, 1211 Geneva 23, Switzerland

Abstract

Since this accumulator has relatively short bending magnets, the fringe-field effects are large, and special attention had to be paid to the tracking of particles through the magnet as well as to its representation in the machine lattice. Here we describe the procedures, making use of measured field tables in computer programs to determine the properties of the machine, and compare predicted machine parameters with measured ones.

1. Motivation for Particle Tracking and Modelling

In an electron ring an accurate knowledge of the lattice functions and of the characteristics of the main elements is essential, as the major properties of the ring, such as beam damping and equilibrium beam parameters, depend on them.

In order to enhance fast damping and accumulation, the Electron-Positron Accumulator (EPA) lattice is based on a highly saturated combined-function bending magnet. A very low bending radius (ϱ = 1.4 m) means large synchrotron radiation-emission in the magnet, and a small gradient ($dB_y/dx = -1$ T/m) favours both injection efficiency and beam stability by an exchange of damping between horizontal and longitudinal planes.

Unfortunately, the combined effect of low bending radius and vertical focusing strength makes the contribution of the fringe-field extension particularly large in so short a bending magnet (ℓ = 0.56 m). Therefore, the magnetic field and its multipolar coefficients, such as gradient and sextupole components, vary both across and along the magnet, and thus along the particle trajectory, and for this an analytical solution is not possible.

For this reason, an ensemble of particle tracking programs (ORBIT and its auxiliary program PREP), based on the exact equation of motion in the measured magnetic field in the median plane, were made with the following aims:

i) to calculate the accurate position and length of the central trajectory through the whole magnet, including fringe-field extension;
ii) to adjust the total length and profile of the magnet pole in order to fit the desired deflection angle and integrated gradient along the real particle trajectory.

In order to maximize the dynamic aperture, we wanted the sextupole component in the magnet to be as small as possible [1]. The magnets were all shimmed [2] to make the integral of the sextupole along the straight length of the magnet close to zero. As the path through the magnet is curved, however, some of the sextupole remains along the orbit. An estimate of this was also made in the preliminary program. The final aim was to have a model of the machine which could be used for quick tracking in programs with an analytical representation of magnetic elements.

2. Steps Leading to the Lattice Parameters and the Final Model

To achieve the above-mentioned requirements, an interleaved use of tracking through field tables (ORBIT and the auxiliary program) and classical lattice programs became necessary. Five steps led from the magnet data to the final model.

1) By tracking orbits around the closed orbit, PREP provided matrix transformations for small betatron oscillations in both the horizontal and vertical planes, for the complete magnet. A pure dipole, with path length LCM was defined [3], which gave the same path length as that found by PREP, and with similar drifts on either side.

2) Considering the magnet with its adjacent drift spaces as a transfer channel, a 'model' channel composed of magnetic elements represented analytically was set up and tuned to the same transfer characteristics. This gave the linear model of the bending magnet.

3) Using this representation of the magnet in the lattice of the full machine in MAD [4], this machine was matched by varying the strengths of the six quadrupole families to satisfy the desired constraints [5] (for example, a desired phase difference over a certain region, working points, etc.).

4) With the resulting quadrupole forces and the machine geometry now defined, the complete machine, with the magnets represented just as in the PREP run, was entered into the full ORBIT program [6], where a special subroutine was added to accept the treated, measured field tables.

Tracking through this lattice gave values for the chromaticities, and for synchrotron integrals for given momenta leading to machine parameters such as energy loss per turn U_0, damping times τ, emittance ϵ_{x0}.

5) Now the linear model was tuned with respect to the chromaticity obtained in step (4), including variations of the magnet end-face rotation ϕ and the sextupole component S. This led to a model satisfying both linear optics and the lowest order of non-linearities.

3. Particle Tracking with ORBIT

3.1 Equations of Motion

If rectangular coordinates are used (a prime denotes differentiation with respect to z), then the exact horizontal and vertical equations of motion are

$$x'' = q[-B_y(1 + x'^2) + y'(B_z + x'B_x)] \quad (1)$$

$$y'' = q[B_x(1 + y'^2) - x'(B_z + y'B_y)] \quad (2)$$

with $q = e/p[(1 + x'^2 + y'^2)^{1/2}]$.

The coordinate z is chosen to be roughly the direction of motion (Fig. 1). For motion purely in the median plane, Eq. (1) reduces to

$$x'' = -e/p[(1 + x'^2)^{3/2}B_y] \, . \quad (3)$$

3.2 Magnetic Data and their Preparation for Tracking

We had at our disposal measured values of B_y in the median plane [2]. Three sets of measurements were made with excitations corresponding to 500, 600, and 650 MeV. In the region of the magnet where the fringe field varies rapidly, we had values on a mesh of $\Delta x = \Delta z = 0.01$ m. In the centre, where the field has a slow variation, and at the edges of the fringe field, there were fewer points. We were supplied with 14 rows of 87 values. Assuming symmetry about the middle of the magnet, by taking averages of points on either side of the centre, we then had 14 rows of 44 values representing half the magnet. Using a CERN Library spline routine we first of all filled in all missing points to give values over a complete mesh every centimetre in x and z over a range of z from 0 to 0.75 m and from -1.15 to 0.5 m in x. By using a combination of the Library routines in LSQ (least squares fit) and SPLIN3, we smoothed the values in order to have as input for ORBIT a set of values of B_y, $\partial B_y/\partial x$, $\partial^2 B_y/\partial x^2$, $\partial B_y/\partial z$, $\partial^2 B_y/\partial z^2$ at every mesh point. The combination of LSQ and SPLIN3 became necessary in order to find smooth second derivatives.

3.3 Tracking through the Magnet

We were then ready to study the basic trajectory (to become the closed orbit in the full machine representation). The central (x = 0) position (see top half of Fig. 1) had been fixed from earlier studies with a simplified hard-edged model. Starting at this central position, with $dx/dz = 0$, we tracked through the second half of the magnet, using Eq. (3). Whenever B_y was required, we used 6 × 6 points to find the interpolated value. A normalization factor (≈ 1) was applied to all the magnetic-field values so that the bending angle was exactly 11.25°. As mentioned before, the horizontal and vertical matrix transformations were calculated, the one for the vertical plane by putting $B_x = y(dB_y/dx)$ and $B_z = y(dB_y/dz)$ in Eq. (2), again always evaluating the field at the point in question along the orbit. Other quantities of interest—such as the trajectory length LT, the integrals of the gradient $\int \partial B/\partial \eta ds$ and of the sextupole $\int \partial^2 B/\partial \eta^2 ds$ were calculated; η is at right angles to the trajectory, s is along it. The results are given in Table 1a.

To get an idea of the confidence level on the estimation of certain magnet parameters, field tables with errors were simulated and orbit runs carried out. Table 1b represents mean values with one r.m.s. error.

Tracking was done for all three sets of magnetic measurements. Some field integrals as a function of particle energy are given in Table 1c; the results show quite well the effect of magnet saturation on the field integrals.

Tracking through the full lattice as mentioned in Section 2, step (4), led to the results given in Table 1d, as well as those in Table 3.

More details can be found in Ref. [7].

4. The Model: Its Fit to Data from ORBIT Runs

The main requirement of the model is to lead to the results of ORBIT for the linear optics and chromaticity when introduced into a lattice program.

Ten parameters, β_x, α_x, μ_x, d_x, d_x/ds, β_y, α_y, μ_y, $\Delta\xi_x$, and $\Delta\xi_y$, the constant total length L, and the C-S invariant are the constraints.

The model has been assembled from two different quadrupoles Q1 and Q2, and one central bending magnet B with thin-lens sextupoles S near the end-faces of this dipole (Fig. 1), from which the main effect of the sextupole stems. Variables to satisfy the above constraints are: the gradients K, K1, K2 of the bending magnet and quadrupoles; the lengths of the elements LC, L1, L2 and of drift space D1, D2, D3; end-face rotation ϕ of the bending magnet; and KS, the force of the sextupole S.

The fitting started with the characteristics of the bending magnet as given by PREP (tracking through the magnet first). The results can be found in Table 2. Despite the high number of constraints, the fit led to sufficiently good agreement between data from ORBIT and the model, so for the sake of simplicity this model was adopted in our machine studies.

It has to be kept in mind, however, that models with higher degrees of element segmentation [8] lead to better fits or allow the inclusion of further constraints.

5. Comparison of Parameters from ORBIT, the Model, and the Real Machine

In the second half of 1986, the EPA commissioning for e^- beams took place [9]. A number of machine parameters directly related to the lattice could be measured at 500 MeV. A comparison between prediction and realization is made in Table 3. The linear optics (Twiss parameters) agrees to better than ± 10%; for only one family of quadrupoles the measured $\int\beta\,ds$ is 18% less than calculated. Figures 2 and 3 illustrate the agreement between prediction and reality. The measured vertical chromaticity ξ_y differs by more than 20% from prediction. Summing up the $\Delta\xi_y$ from the different elements in the lattice reveals that the major part of ξ_y stems from the bending magnet whose sextupole component could be estimated with a large tolerance only (see Table 1). In addition, its calculation was done with respect to an ideal closed orbit (orbit distortions of ~ 7 mm have been observed). These facts may, to a good extent, explain the discrepancy.

6. Applications of the Model

The model has been used in a wide range of lattice programs to study
- trajectories,
- closed-orbit deformations (e.g. ejection),
- dynamic apertures at the different energies and sextupole forces in the bending magnet.

Its main application is, however, to be found in the lattice program used for on-line modelling [10]. Here, thanks to the good agreement between machine parameters of the model and the real machine, it has eased machine studies at commissioning and finds its application in day-to-day operation.

Acknowledgements

We are very much indebted to D. Cornuet, G. Suberlucq and M. Tardy for their work on the magnets. Without their very careful measurements our result would have been impossible.

Table 1
Some magnet and lattice data gathered from ORBIT and PREP runs

Tracking range = D/2: $0 \le z \le 0.750$ m (see Fig. 1).
Averaging over full range $B(z) = [B(z) + B(-z)]/2$.
For (a), (b), (d) the particle energy of the EPA is E = 500 MeV.

a) Results deduced from the field table as provided by measurements of the magnet

Central field B(xyz = 0):	1.16171 T
Central gradient G(xyz = 0):	−0.990992 T/m
Central sextupole S(xyz = 0):	1.69414 T/m²
Integrals of field ∫B ds:	0.654956 T•m
Gradient $\int\partial B/\partial\eta\,ds$:	−0.867060 T
Sextupole $\int\partial^2 B/\partial\eta^2 ds$:	0.28688 T/m
Length of magnet for which the matrix has been calculated (LCM):	0.590448 m
Length of trajectory with D = 1.5 m:	LT = 1.521680 m
Distance of basis D to centre of magnet:	X1 = −0.106548 m
Max. swing of trajectory around x = 0:	X0 = 0.013503 m

Elements of transfer matrix:

H_{11} = 1.0810005	V_{11} = 0.8500136
H_{12} = 0.5944441	V_{12} = 0.5707717
H_{21} = 0.2834486	V_{21} = −0.4861429
H_{13} = 0.1163174	
H_{23} = 0.4072015	

b) Three field characteristics taking into account tolerances of positions and Hall probe (simulation of field tables with errors)

Integral of gradient $\int\partial B/\partial\eta\,ds$:	−0.86755 ± 0.00373 T
Integral of sextupole $\int\partial^2 B/\partial\eta^2 ds$:	0.14 ± 0.49 T/m
Distance of basis D to centre of magnet X1:	−0.10654 ± 0.00006 m

c) Some field integrals as function of particle energy

Energy (MeV)	∫B ds (T•m)	$\int\partial B/\partial\eta\,ds$ (T)	$\int\partial^2 B/\partial\eta^2 ds$ (T/m)
500	0.654956	−0.86755 ± 0.00373	0.14 ± 0.49
600	0.785946	−1.03320 ± 0.00440	−0.16 ± 0.58
650	0.851440	−1.10480 ± 0.00470	−0.60 ± 0.64

d) Results from ORBIT runs of full machine structure

- Synchrotron integrals, sextupole in bending magnet = 0.28688 T/m, correcting sextupoles off:

$\Delta p/p_0$	−0.009	0.0	0.010
I_1	3.968	4.224	4.552
I_2	4.072	3.960	3.843
I_3	2.755	2.643	2.524
I_4	−4.706	−4.161	−3.611
I_5	2.034	1.976	1.956

- Chromaticity: $\xi_x = -1.31$, $\xi_y = -1.81$.

Table 2
Parameters of the model as used in the lattice (E = 500 MeV)

Bending magnet B:

LC = 0.6202850 m
K = −0.72801 m⁻²
α = 0.39270 rad
φ = 0.0 rad

Quadrupole Q1: L1 = 0.0137440 m; K1 = −2.28743 m⁻²

Quadrupole Q2: L2 = 0.0088220 m; K2 = −0.34837 m⁻²

Sextupole S: LS = 0.0000090 m; KS = 25880.5 m⁻³

Drift spaces:

	L (m)
D0:	0.0000010
D1:	0.1068970
D2:	0.0135132
D3:	0.2888713

Table 3
Machine parameters as obtained from ORBIT, the model, and measurements

Parameter	ORBIT	Model	Machine	Remarks
Q_x	4.458	4.460	4.430	
Q_y	4.379	4.380	4.390	
d_x (m)	2.301 (max.)	2.299 (max.)	d_x model: ±8%	1
d_y (m)	0	0	0 ± 0.011	
$\int\beta_x ds$ (m²)		7.53–38.18	$\int\beta_x ds$ model: $^{+3}_{-10}$ %	2
$\int\beta_y ds$ (m²)		4.64–55.58	$\int\beta_y ds$ model: $^{+0}_{-18}$ %	
Δx (mm)		±10 (max.)	Δx model: ±0.7	3
Δy (mm)		±6 (max.)	Δy model: ±0.7	
ξ_x	−1.32 ± 0.12	−1.31	−1.16 ± 0.07	4
ξ_y	−1.77 ± 0.40	−1.81	−2.23 ± 0.14	
U_0 (keV)	3.50	3.50	3.50 Ref. [11]	
ϵ_{x0} (μrad•m)	0.089	0.082	0.092	5
τ_x (ms)	58.7	56.5	62 ± 5	
τ_y (ms)	120.3	119.8	119 ± 5	
τ_ϵ (ms)	126.7	136.2	130 ± 10	

Remarks:
1) Comparison is made for measurements at magnetic pick-ups, Ref. [12].
2) Deduced from ΔQ = F(ΔK); Δ(K) from six families of quadrupoles.
3) Orbit distortions generated by horizontal and vertical dipoles with maxima as indicated.
4) Model adapted to a sextupole component of 0.287 T/m per bending magnet (Table 1).
5) Deduced from ϵ_{xc} = 0.083 μrad•m, ϵ_{yc} = 0.0089 μrad•m. All values are for low beam current.

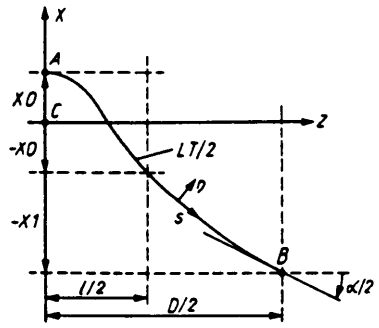

C centre of magnet (X=Z=0)
D tracking range
l phys length of magnet
X1 distance between axis X=0 and B where the trajectory leaves the field
LT = 2 ≡ $\widehat{AB}$ length of true trajectory
XO max swing of trajectory around X=0

Schematic drawing of 1/2 magnetic with fringe field region as used for ORBIT runs (difference arc/trajectory exaggerated)

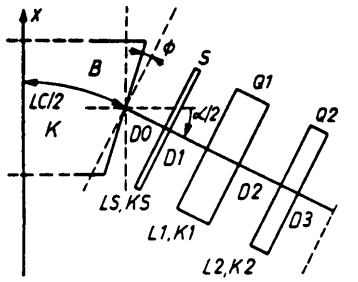

B bending magnet
Q1,2 quadropoles
S sextupole
K,K1,2 gradients (m^{-2})
KS sextupole component (m^{-3})
LC,LS } lengths (m)
DO,1,2,3 }
L1,2 }
φ endface rotation
α bending angle (=22.5°)

Schematic drawing of 1/2 magnet as used as model

Fig.1: AN ARTIST'S VIEW OF THE PARTICLE TRAJECTORY WITH MAGNET AND ITS MODEL

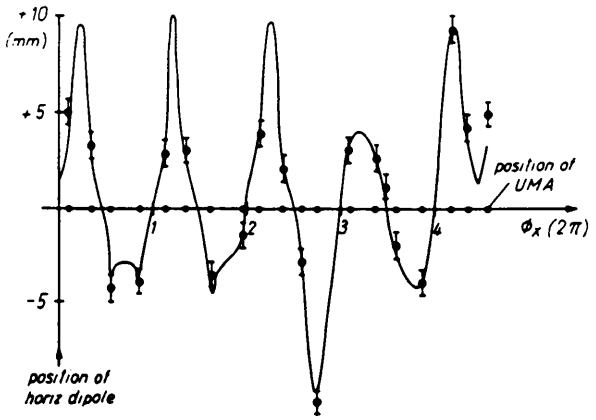

Δx at pick-ups (UMA) when horizontal kick = +1.39 (mrad)

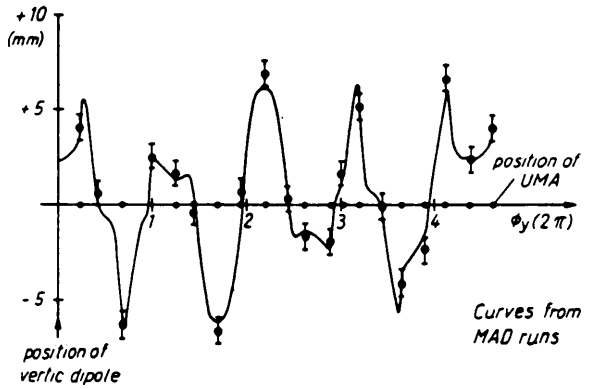

Δy at pick-ups when vertical kick = + .86 (mrad)

Fig.3: COMPARISON OF CALCULATED (MODEL) AND MEASURED CLOSED ORBIT PERTURBATIONS

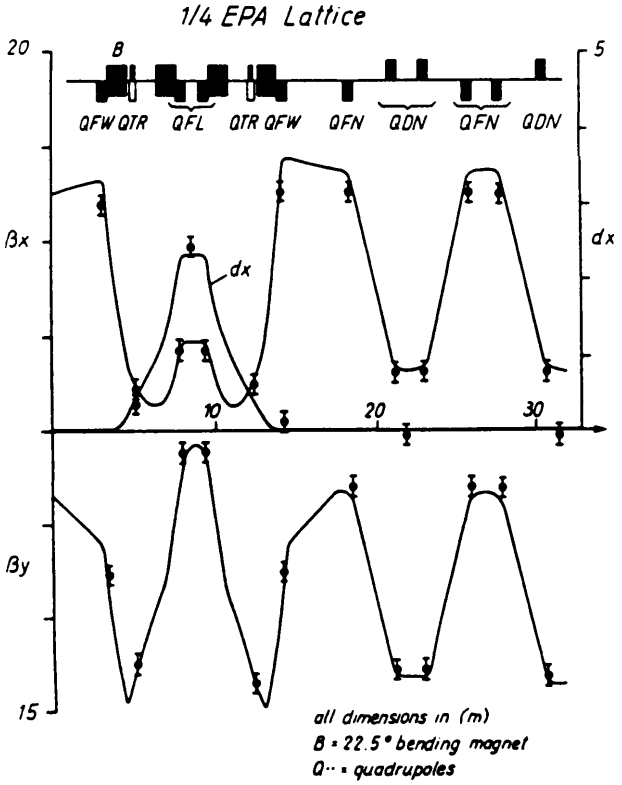

Fig.2: COMPARISON OF BETA AND DISPERSION FUNCTIONS OF MEASUREMENTS AND MODEL

References

[1] S. Battisti et al., Proc. 12th Int. Conf. on High-Energy Accelerators, Batavia, 1983 (FNAL, Batavia, Ill., 1983), p. 170.
[2] G. Suberlucq and M. Tardy, Mesures magnétiques des dipôles EPA type 1, CERN PS/PSR/Note 86-6 (1986).
[3] J.P. Delahaye, EPA geometry, CERN PS/LPI/Note 83-27 (1983).
[4] Ch. Iselin, The MAD Program, CERN-LEP/TH/86-15 (1986).
[5] J.P. Delahaye and A. Krusche, The LEP Electron Positron Accumulator basic parameters, LEP Note 408 (1982).
[6] B. Autin and M. Bell, ORBIT program document, in preparation.
[7] M. Bell and H. Kugler, The EPA bending magnet and its representation in the full description of the machine, CERN PS/LPI/Note 86-01 (1986).
[8] H. Kugler, *in* CERN Workshop on Computer Programs for Accelerator Lattice Calculations, April 1986.
[9] J.H.B. Madsen et al., First experience with the pre-injector (LPI) by the LPI Beam Commissioning Team, these Proceedings.
[10] J.P. Delahaye et al., On-line modelling, a tool at commissioning of the 600 MeV e^+/e^- accumulator (EPA) of LEP, these Proceedings.
[11] S. Bartalucci, CERN, private communication.
[12] S. Battisti et al., Magnetic beam-position monitors for the LEP pre-injector (LPI), these Proceedings.